Encapsulation of Nano Disperse Red 60 via Modified Miniemulsion Polymerization. I. Preparation and Characterization

Galila M. El-sayed,[1] M. M. Kamel,[2] N. S. Morsy,[1] F. A. Taher[1]

[1]*Department of Physical Chemistry, Faculty of Science (Girls), Al-Azhar University, Egypt*
[2]*Textile Research Division, National Research Center, Egypt*

Received 18 December 2009; accepted 14 June 2011
DOI 10.1002/app.35102
Published online 12 January 2012 in Wiley Online Library (wileyonlinelibrary.com).

ABSTRACT: Nanocolorant, nano Disperse Red 60, was successfully prepared via modified miniemulsion polymerization process. Transmission electron microscopy was employed to determine the droplet and particle sizes. The effects of the speed and the time of homogenization, the surfactant nature and its amount, the presence of dye, the initiator nature, and the presence of a crosslinker on the morphology and particle size of nanocolorant were studied. UV–vis absorption spectra of nanocolorant with respect to the commercial corresponding dye showed a hypsochromic shift confirming the decrease in particle size. Fourier transform infrared spectra proved the chemical composition of nanocolorant particles assisting the incorporation of the dye within the polystyrene particles. The monomer conversion, surface tension, and apparent sedimentation stability also were measured. The relative electrical conductivity of the suspension was used for determining the polymerization mechanism. The kinetic polymerization was investigated using a pseudofirst-order and it is found that the rate constant of polymerization equals 0.01358 min^{-1}. Zeta potential measurements were employed for miniemulsion which showed that it has good stability at all range of pH. © 2012 Wiley Periodicals, Inc. J Appl Polym Sci 125: 1318–1329, 2012

Key words: modified miniemulsion polymerization; dispersion; nanocolorant; polymer; kinetic analysis; conductivity

INTRODUCTION

Dyestuff and pigment particles have been largely used in laser materials,[1] optical disks,[2] nano-scale semiconductor devices,[3] colorants for textile products, inks, and coatings.[4] However, because of the respective inherent disadvantages of dyestuffs and pigments, they cannot meet the need for better performance and lower cost for an increasing number of applications. Thus, nanocolorants have been developed as a new class of colorants that can achieve the advantages of both dyestuffs and organic pigments.[5] The encapsulation of the dyes within polymer to produce nanocolorants can solve the agglomeration problem in the aqueous phase and also protect them from unwanted environmental influences like UV radiation or pH. Moreover, the encapsulation leads to better storage, thermal, and color stability and superior durability. Therefore, polymer-encapsulated dyes could find applications in a wide range.[6]

To encapsulate the dye into polymer latex particles, the chemical methods of polymerization and electrohydrodynamic atomization[7] were widely used. Polymerization methods have many types such as: suspension polymerization,[8] dispersion polymerization,[9] emulsion polymerization,[10] soap-free emulsion polymerization,[11] miniemulsion polymerization,[12,13] and microemulsion polymerization.[14] In recent years, a large number of nanohybrid particles were prepared by miniemulsion polymerization because of its attractive advantages.[15–17] Miniemulsion polymerization is a convenient way to incorporate dyes of poor water solubility into polymer nanoparticles.[18,19] It is an aqueous dispersion of a relatively stable oily droplets prepared by ultrasonication or homogenization of a system of oil/water, surfactant and highly water-insoluble compound, a so-called hydrophobe whose function is to restrict degradation of droplets (Ostwald ripening).[20] Ostwald ripening of the droplets is a phenomenon where large particles grow larger at the expense of smaller particles dissolving in the polymerization medium.

Particle formation in an emulsion polymerization reaction can be proceeded by one or more of the following mechanisms: micellar nucleation, homogeneous nucleation, and droplet nucleation.[21,22] It was known that in miniemulsion polymerization, particle nucleation mechanism depends on droplet nucleation and homogeneous nucleation. The droplet nucleation mechanism suggests that the droplets

Correspondence to: M. M. Kamel (mona_kamel_nrc@yahoo.com).

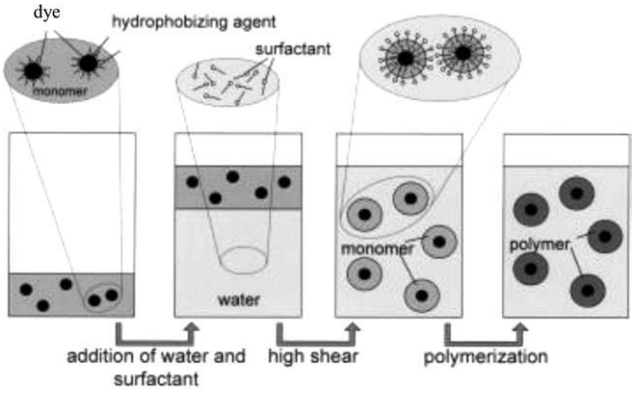

Figure 1 Principle of encapsulation bymodified miniemulsion polymerization.

formed during the emulsification step are polymerized directly via a radical that enters these monomer droplets and reacts with the monomer present there. The homogeneous nucleation is a second possible mechanism for miniemulsion polymerization. In this case, the latex seeds are created from oligomers in the water phase and the monomer is brought to the nucleation site by diffusion. One of the advantages of the miniemulsion polymerization technique is encapsulation of nanoparticles that can be carried out via directly dispersing the hydrophobic inorganic particles in the monomer phase and nucleating all the droplets containing inorganic particles in miniemulsions.[23,24]

The basic requirements of dyes to be suitable for the introduction into minidroplets are high hydrophobicity, high solubility in monomer, and large absorption coefficient. In this case highly hydrophobic anthraquinone-based disperse dye was used, so the used dye itself just acted as good hydrophobe to prevent the minidroplets from Ostwald ripening.[25] In addition, to ensure the enhancement of light stability of both matrix polymer and dye, we introduced the well-compatible light stabilizer into minidroplets to make nanocolorant structurally photostable.[26,27]

Quite few approaches have been briefly reported to prepare nanocolorants. For instance, copper phthalocyanine dye and styryl dye have been encapsulated into polystyrene latex using miniemulsion polymerization to get colored latex particles.[28–30] A modified miniemulsion process was reported to prepare a nanocolorant by one-step miniemulsion polymerization, see Figure 1,[31] based on the architecture which originally was designed, and the practical performances of the obtained nanocolorant were well characterized. A set of so-called nanocolorants consisting of crosslinked polystyrene with solvent yellow, red, and blue dyes has been produced via a modified miniemulsion polymerization process.[5,32]

For all the above cases, the dyes have good solubility in monomers, which is attributed to the successful preparation of colored latex with particle size larger than 50nm. However, as for those oil-soluble dyes with poor solubility in monomers, their improvement of the water dispersibility via miniemulsion polymerization is rarely involved. So, our trail involved the preparation of nanocolorant that is sparingly monomer-soluble dye to achieve excellent stability of colloidal dispersion with smaller particle size and higher monomer conversion of nanocolorant. In this work, we aim to utilize modified miniemulsion polymerization for preparation and characterization of nanocolorant particles. We have studied several reaction parameters, including the speed and the time of homogenization, the surfactant nature and its amount, the presence of dye, the initiator nature, and the presence of a crosslinker, to assess the influence of these factors on the final latex particles.

EXPERIMENTAL

Materials

Anthraquinone-based disperse red dye (Dianix Classic Red FB; C.I. Disperse Red 60, DR60, $M_w = 331.3$, DyStar) was used as the essential material, the molecular structure is shown in Scheme 1. Scanning electron microscope (SEM) image of DR60 is shown in Figure 2. Styrene (ST, 99.5%, Merck), and Methyl methacrylate (MMA, 99%, Merck) were used as monomers. Divinyl benzene (DVB, 80%, Fluka) and glycol dimethacrylate (GDMA, 98%, Bio-Rad) were used as crosslinkers. Polystyrene (PS, Merck, molecular weight = 50,000) was used as a hydrophobe. Sodium dodecyl sulfate (SDS, 99%, Merck), cetyl trimethyl ammonium bromide (CTAB, Merck), and Ultravon PL (UPL, Ciba) were used as surfactants. Reactive hindered amine light stabilizer (RHALS, Clariant) was used as a stabilizer.

Potassium persulfate (KPS, Cambrian chemicals) and 2,2-azobis(2-methyl propionitrile) (AIBN, Aldrich) were used as initiator. Hydroquinone (HQ, Aldrich) was used as an inhibitor. Sodium hydrogen carbonate (NaHCO3, Fluka), sodium chloride (NaCl, Merck), and potassium bromide (KBr, Aldrich) were of analytical grade. Nitrogen purified with silica gel and molecular sieve was used to remove oxygen from the reaction mixture. All the chemical reagents were used as received.

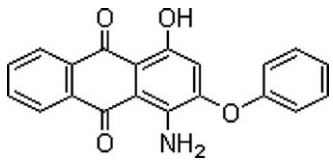

Scheme 1 C.I. Disperse Red 60.

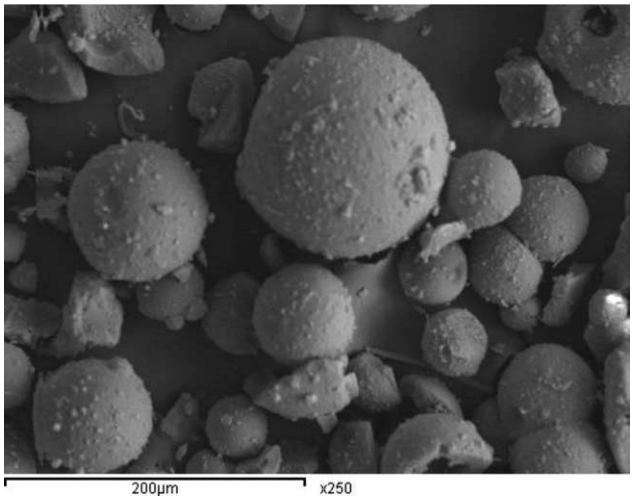

Figure 2 SEM of C.I. disperse Red 60 before conversion to nanosize.

Preparation of nanocolorant

The recipe used for the synthesis of nano C.I. Disperse Red 60 (nDR60) particles via modified miniemulsion polymerization[32] is summarized in Table I.

As cited in Table I, the miniemulsion was prepared by dissolving SDS and $NaHCO_3$ in deionized water while DR60, RHALS and predissolved PS in the oily solution. The oily and aqueous solutions were mixed and quickly stirred (200 rpm) at room temperature for 20 min to obtain a completely homogeneous macroemulsion. The resultant macroemulsion was miniemulsified with a homogenizer (WiseMix^{TM} Digital Homogenizer HG 15D, Korea.) for different time intervals under ice cooling. Then the miniemulsion was transferred into a flask equipped with agitator, thermometer, reflux condenser, conductivity meter, and nitrogen spurge tube. The system was purged with nitrogen for 10 min and heated to 60°C under nitrogen flow, simultaneously stirring by paddle stirrer at 200 rpm to avoid any oxygen content inside the flask. The polymerization was started by injecting an initiator at 60°C followed by temperature increase at 1°C min^{-1} to 70°C. The reaction temperature was held at 70°C for 4 h to achieve a complete conversion.

Samples were withdrawn periodically every 30 min with a pipette from the middle zone of flask and then short-stopped with a 2% aqueous hydroquinone solution. The samples were freeze-dried and the rest was used to determine monomer conversion gravimetrically. The weight of polymer was calculated by subtracting the known weights of surfactant and hydroquinone from the total weight of the freeze-dried samples.

Analysis and characterization

Scanning electron microscopy was performed with JEOL (SEM-840A, Japan), operating at acceleration voltage of 80 kV. Particle samples were spread onto copper wafer and subsequently sputtered with 250A° of gold before testing. Transmission electron microscopy was performed with JEOL (TEM-1230, Japan), operating at acceleration voltage of 100 kV. Samples dispersed in deionized water were transferred to carbon coated copper grids and left to dry before testing. The particle size distributions of the aqueous suspensions were determined by a dynamic light scattering instrument, DLS, (NICOMP 380, ZLS, USA). A laser Zetameter (Malvern Instruments model Zetasizer 2000, United Kingdom) was employed for zeta potential measurements. 0.01 g of samples was placed in 50 mL deionized water at ionic strength of 2×10^{-2} *M* NaCl. The pH was then adjusted to the required value. The samples were shaken for 30 min. After shaking, the equilibrium pH was recorded and the zeta potential of the sample particles was measured. A Fourier transform infrared spectrometer (FTIR Shimadzu, Japan) was used to determine the chemical structure. UV–vis absorption spectra were studied using a UV–vis spectrophotometer (Perkin–Elmer Lambda 35, USA). The electrical conductivity of the suspension was measured using conductivity meter (JENWAY 4510, England). The surface tension was measured using a tensiometer (KRÜSS Tensiometer K6, Germany). The apparent sedimentation stability was assessed by measuring the sedimentation speed of DR60 and nDR60 with the aging time. These samples were located into a glass tube of 0.5-cm inner diameter and 20-cm length.

RESULTS AND DISCUSSION

Factors affecting preparation of colored latex particles via modified miniemulsion polymerization

Effect of homogenization speed

The mean monomer droplet size is significantly correlated with agitation speed. The agitation speed was varied from 5000, 10,000, 20,000 to 24,000 rpm

TABLE I
Representative Recipe Used to Prepare nDR60

Ingredient	Concentration
ST	80 wt %[a]
MMA	12 wt %[a]
DVB and GDMA (1 : 1)	8 wt %[a]
DR60	40 wt %[a]
SDS, UPL, CTAB	20–80 mmol[b]
$NaHCO_3$	10 mmol[b]
KPS, AIBN	10 mmol[b]
Deionized water	78–79 wt %[c]
PS	0.2 wt %[c]
HV 3050	0.15 wt %[c]

[a] Based on the monomer 12.5 g.
[b] Based on the aqueous phase.
[c] Based on the total recipe.

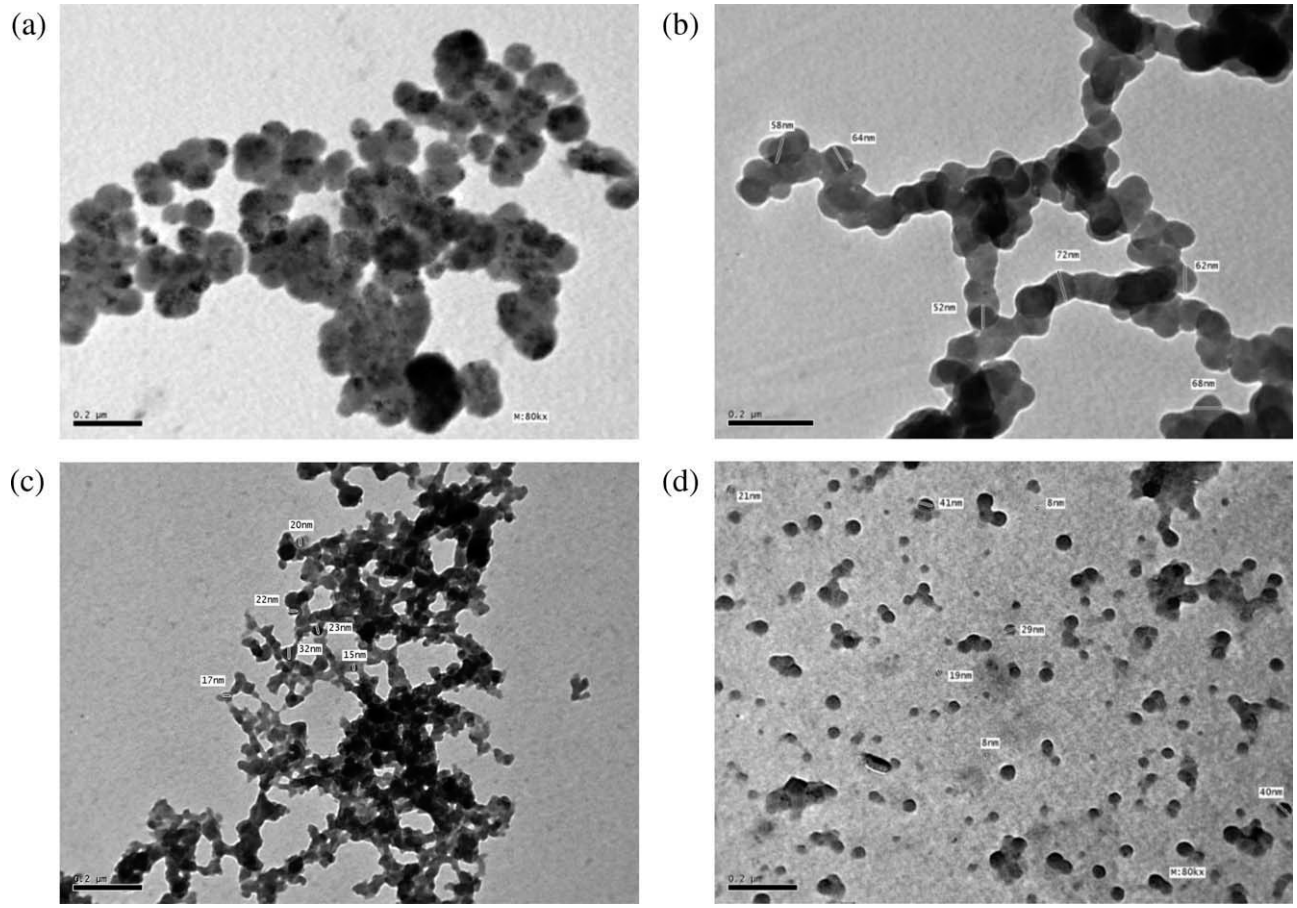

Figure 3 TEM images of the prepared nDR60. (a) 5000 rpm, (b) 10,000 rpm, (c) 20,000 rpm, before polymerization, (d) 20,000 after polymerization, ([SDS]: 80 mmol, 20 min, [nDR60] = 50 g L^{-1}).

to assist the formation of monomer droplets. The corresponding TEM images of the prepared nDR60 exhibit a regular spherical shape, with decrease in droplet size to 8–40 nm as agitation speed increases to 20,000 rpm [Fig. 3(a–c)]. This result indicates that high agitation speed results in significant reduction of the monomer droplet size, which is correlated with the size of the final colored latex product [Fig. 3(d)]. The optimum agitation speed is 20,000 rpm which resulted in a minimum droplet size with higher stability and more uniform spherical particles. However, at 24000 rpm, the excessive intense shearing force unfavorably made surfactant molecules desorbed from nanoparticles (TEM image was not shown) and lowered the sedimentation stability of miniemulsion from 99% corresponding to 20,000 rpm to 87% at 24,000 rpm.

Effect of homogenization time

The effect of agitation time on the monomer droplet size of nDR60 was checked as shown in Figure 4. It can be seen that droplet size decreased when the agitation time initially increases from 5, 10, 15, to 20 min and after that approaches a steady value. During the early stage, there are sufficient surfactant molecules available for stabilizing the newly created surface in the system. Hence the droplet coalescence can be effectively retarded and the droplet size decreases dramatically. As the process proceeds, a large amount of surfactant molecules dissolved in water is rapidly consumed and the role of the droplet coalescence becomes important. Finally, when the equilibrium between the fission by agitation and fusion by collisions is established, the droplet size shows a little dependence on the agitation time and reaches a plateau when the agitation time is longer than 20 min. The longer shearing time generates a significant amount of heat, even under ice cooling, which harms the sample being emulsified and lowered the sedimentation stability of miniemulsion from 99% at 20 min to 91% at 30 min, Table II.

Effect of type and concentration of surfactant

The type and concentration of the surfactant are two of the process variables that determine the morphology properties of the colored latex.[33] Three representative kinds of surfactants: anionic surfactant SDS, cationic surfactant CTAB, and nonionic surfactant

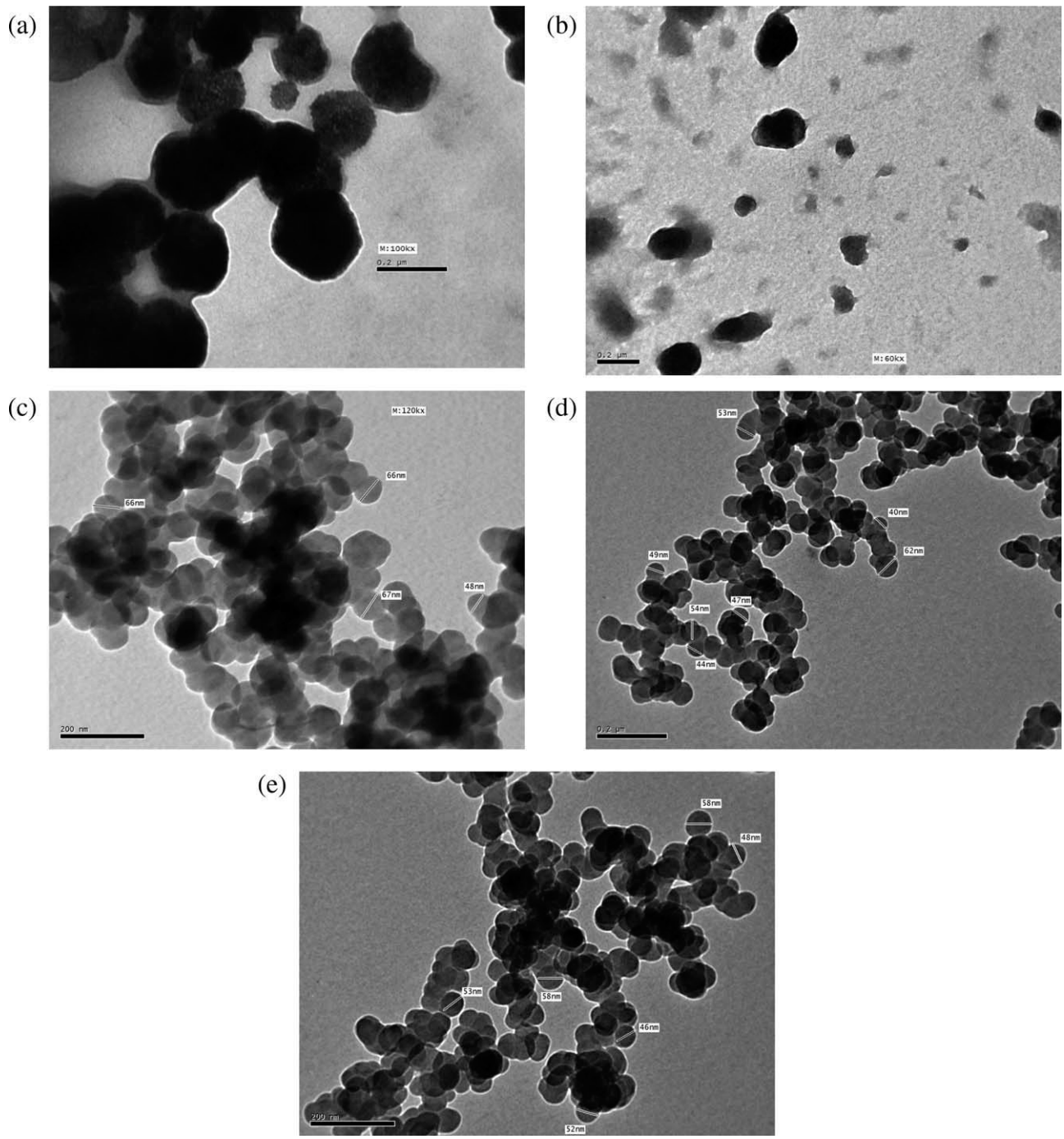

Figure 4 TEM images for the influence of homogenization time on the droplets size of nDR60. (a) 5 min, (b) 10 min, (c) 15 min, (d) 20 min, and (e) 30 min, ([SDS]: 80 mmol, 20,000 rpm, [nDR60] = 50 g L^{-1}).

UPL were compared to get a stable miniemulsion with higher monomer conversion. As shown in Figure 5, SDS and CTAB can assist the formation of stable miniemulsion while nonionic one cannot, because of their different stabilization mechanisms.[34] SDS and CTAB provide the colored latex with electrostatic and steric effects realizing good stabilization. While UPL has only the steric effect that unable to stabilize the whole system, then phase separation occurs. As shown in Table III, the sedimentation stability and the monomer conversion of miniemulsion with SDS are higher than that of the miniemulsion with CTAB. Possibly because, as initiating the polymerization process, the negatively charged sulfate end groups ($-SO4^-$) originating from the persulfate of SDS molecules act as an electrostatic stabilizer that impart higher conversion and higher colloidal stability of the colored latex particles.

The nanocolorant particle size can be varied over a wide range by changing the amount of SDS.

TABLE II
The Influence of Homogenization Time on the Droplets Size of nDR60[a]

Agitation time (min)	Droplet size (nm)	Sedimentation stability[b] (%)
5	250–150	–
10	200–100	–
15	75–50	–
20	65–40	97
30	60–45	91

[a] ([SDS]: 80 mmol, 20,000 rpm).
[b] Sedimentation stability was checked for 60 days.

As shown in Figure 6, by increasing the amount of SDS from 20, 40, 60, to 80 mmol, the droplet size decreases to $\sim$ 20 nm. This is because more SDS molecules are available for stabilizing the oil/water interface area generated during homogenization time at higher concentration and also the coalescence among monomer droplets is reduced. However, the amount of SDS should be limited under the critical micelle concentration (i.e., [SDS]CMC = 87.65 mmol)[35] to avoid micellar nucleation during the polymerization.[36] The determined residual concentration of SDS in the water phase was less than the CMC that indicates there are no micelles in the water phase.

Effect of the presence of dye

The amount of the hydrophobic dye dissolved in ST plays an important role in the stability and phase separation between the polymer and dye during the polymerization process.

For a small dye loading, the intermolecular interaction of the dye is weak because of the relatively large intermolecular distance, and the rate of polymerization of monomers is thought to be higher than the clustering rate of dye molecules. Thus, it is difficult to obtain complete phase separation, but the dye molecules basically attached to the macromolecular chains. Hence, suppressed Ostwald ripening from the hydrophobic dye will not likely be enough to generate a highly stable miniemulsion and also will lead to inadequate color depth for nanocolorant. Along with an increasing feed amount of the dye, the enhanced intermolecular interaction of the dye molecules and reinforced hydrophobic action of the

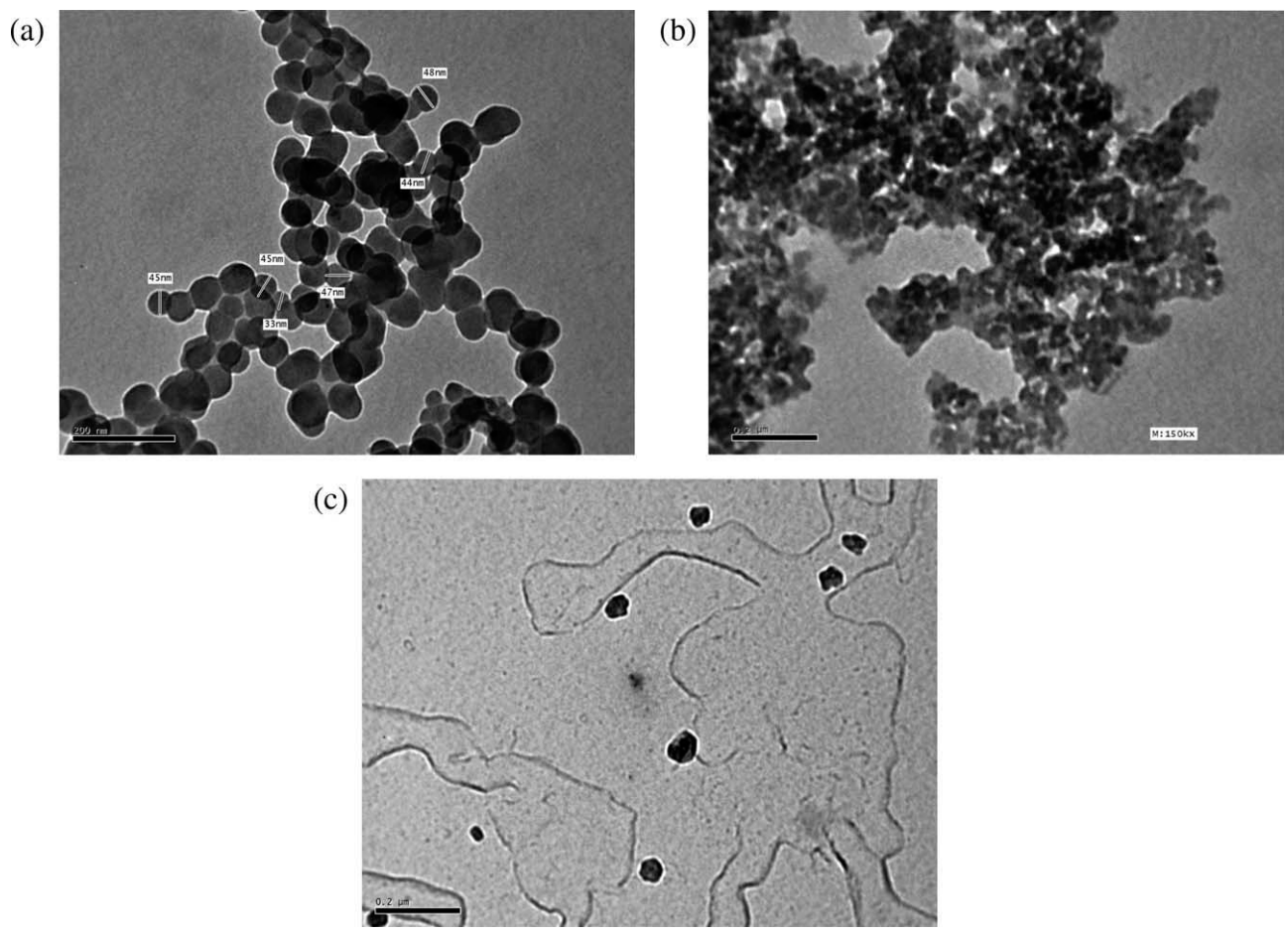

Figure 5 TEM images for the effect of surfactant types on the droplet size of nDR60. (a) SDS, (b) CTAB, and (c) UPL ([surfactant]: 80 mmol, 20,000 rpm, 20 min, [nDR60] = 50 g L^{-1}).

TABLE III
Characterization of Surfactants Used in Modified Miniemulsion Polymerization

Surfactants	Type	Sedimentation stability[a] (%)	Monomer conversion (%)	CMC[b] (mol)
SDS	Anionic	97	99	8.76×10^{-3}
CTAB	Cationic	85	75	0.92×10^{-2}
UPL	Nonionic	Phase separation	–	1.30×10^{-2}

[a] Sedimentation stability was checked for 60 days.
[b] CMC in water at 25°C.

dye promote phase separation when monomers originally acting as solvents turn into polymers. Consequently, besides a fraction of the dye attached to the macromolecular chain, more dye forms a separated dye phase and tends to be embedded in the polymeric interior. However, if the dye overloads, when the monomer droplets turn into polymer particles with a smaller volume, the excessive dye will likely be expelled from the polymeric layer by phase separation and forms an agglomerate to settle down. Moreover, overloaded dye makes a thinner polymer layer and weakens the packaging ability of the polymer; thus, the migration of the dye incorporated into the polymer will be accelerated.[5,26]

To account for this result, the dye solubility was determined gravimetrically at 25°C after separation of the insoluble part by centrifugation. DR60 concentration in ST was found to be equal to 50 g L^{-1} at saturation. Consequently, the miniemulsion polymerization was performed in the presence and in the absence of DR60 50 g L^{-1}. As shown in Figure 7, the solublized red dye contributes to retardation of Ostwald ripening by increasing osmotic pressure in the monomer droplets and has a significant effect on the morphology of the nanocolorant.

Effect of polar monomer and crosslinker

To achieve integrated morphology of nanocolorants, based on water-insoluble nonpolar, ST, it is very important to introduce a proper amount of polar monomers. Polar MMA and GDMA, which also act as a crosslinker, were used. The effect of adding polar monomers as a constituent of miniemulsion on the morphology of nanocolorant can be observed in

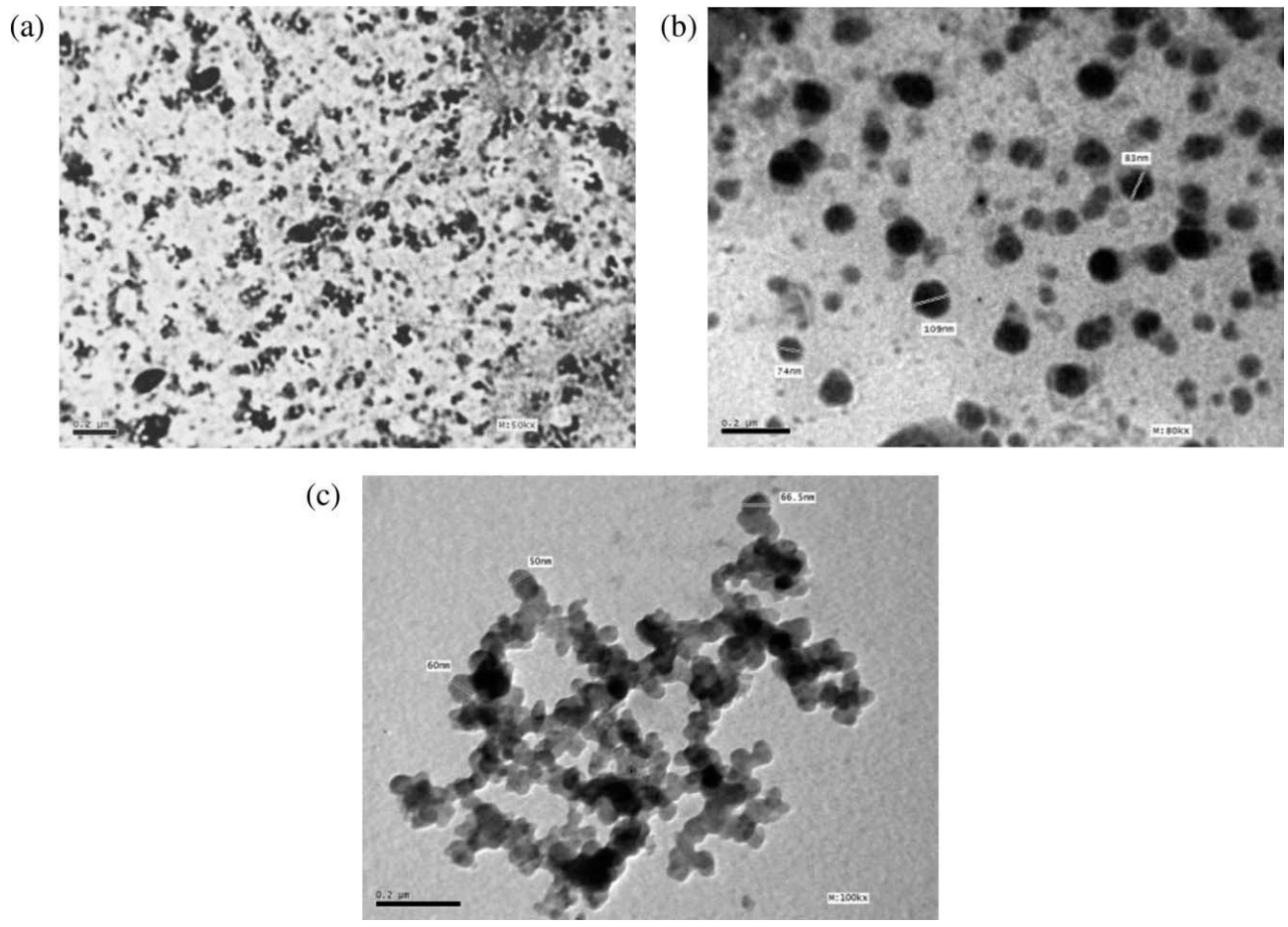

Figure 6 TEM images for the effect of SDS concentration on the droplet size and morphology of nDR60. (a) 20, (b) 40, (c) 60, (d) 80 mmol (20,000 rpm, 20 min, [nDR60] = 50 g L^{-1}).

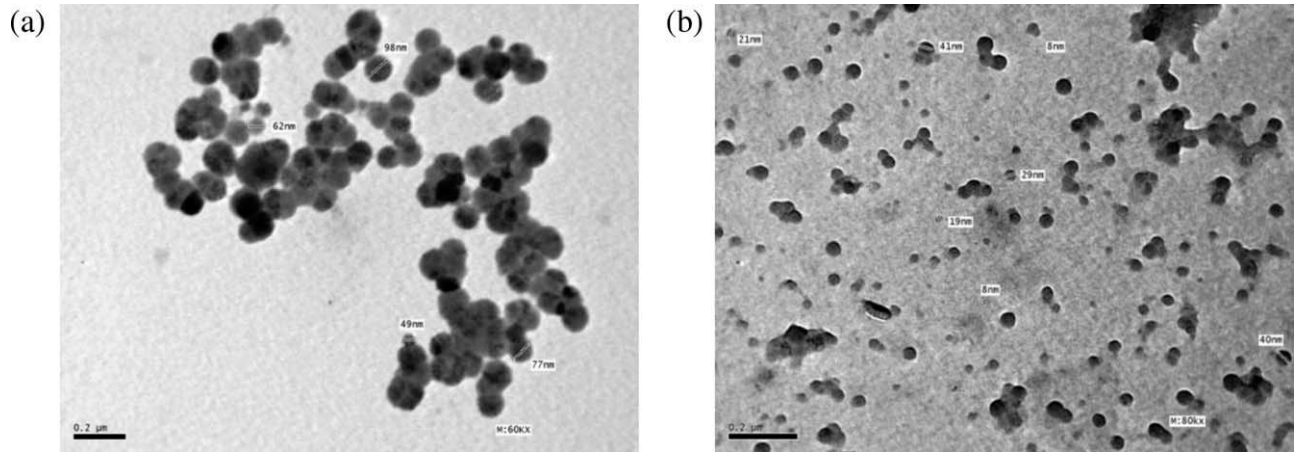

Figure 7 Effect of the presence of DR60 on the droplet size. (a) [DR60] = 0, (b) [DR60] = 50 g L^{-1} ([SDS] 80 mmol, 20,000 rpm, 20 min).

the TEM images in Figure 8. The nanoparticle surfaces without polar monomers are not as even as that in the presence of polar monomers. This is because of the incomplete surfactant molecules coverage for minidroplets, where the surface tension of nDR60 (39 mN m^{-1} at 25°C) lies above that of saturated SDS (17 mN m^{-1} at 25°C). In the presence of MMA and GDMA in minidroplets, both tend to concentrate in oil/water interface region because of their higher hydrophilicity and to further lower the interfacial energy. Subsequently, the high hydrophobic dye was impelled into the inner region of minidroplets.

Accordingly, it facilitated the crosslinked polar polymer, GDMA, to mainly locate on the outer layer of nanoparticle and made the dye to embed in the interior of nanoparticle during the polymerization process; consequently, the nanocolorant particles obtained a modified polarity and surface property. Thus, the moderate crosslinking density for polymer is indispensable. In addition to GDMA crosslinker, a proper amount of DVB was added. Because the crosslinker can lead the more compact polymeric exterior and greatly reduces the free volume of the polymer; accordingly, the dye molecular migration from the polymeric matrix is sharply restrained. Total amount of crosslinkers content should be limited to 10 wt % with respect to the monomer to prevent the heterogeneity of the polymeric matrix due to their tendency toward self-polymerization. The difference in the morphology of nanocolorant prepared with and without crosslinker was observed in Figure 9. The crosslinked one shows more rigid and compact polymer with larger reduction in the droplet size than the corresponding one without crosslinker.

Effect of initiator type

Two types of initiators were used in modified miniemulsion polymerization, water-soluble initiator (KPS) and oil-soluble initiator (AIBN), to see which initiator could be more suitable for initiating the modified miniemulsion polymerization. The

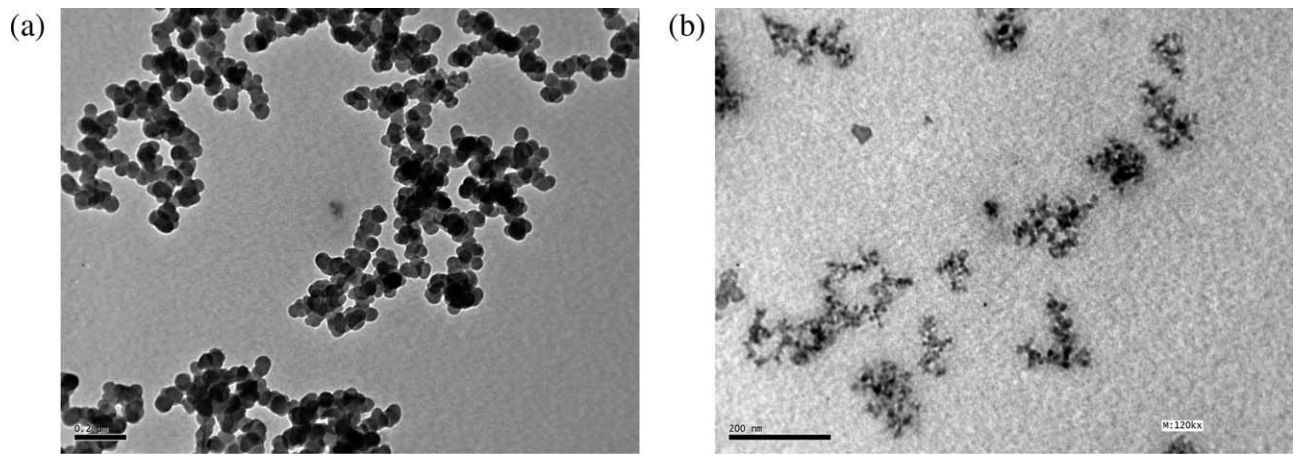

Figure 8 TEM images for nDR60. (a) with, (b) without polar monomers (20,000 rpm, 20 min, [SDS]: 80 mmol, [nDR60] = 50 g L^{-1}).

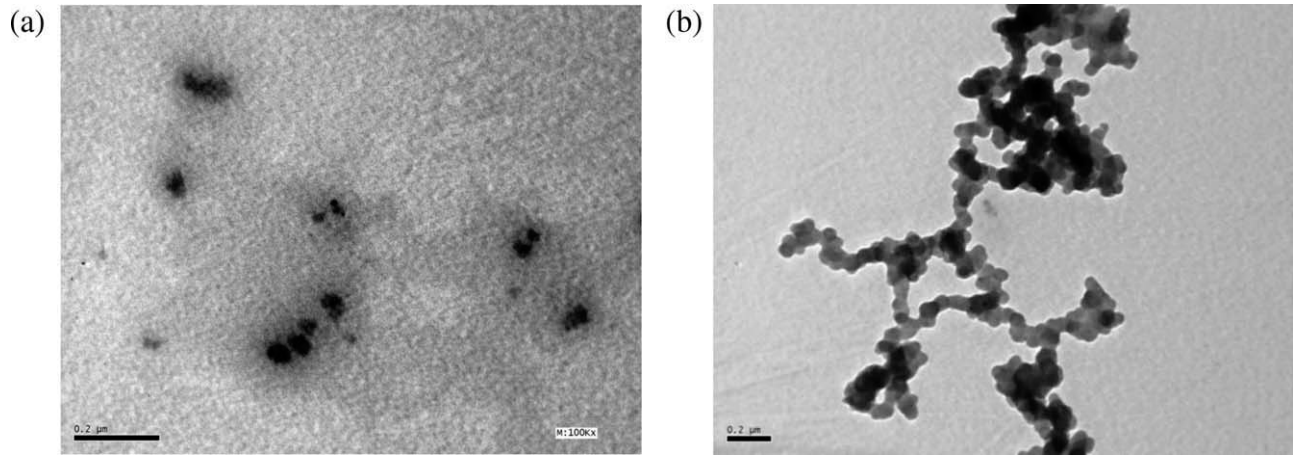

Figure 9 TEM images for the effect of crosslinker on the droplet size of nDR60. (a) [crosslinker] = 0, (b) [crosslinker] = 8 wt % ([SDS]: 80 mmol, 20,000 rpm, 20 min, [nDR60] = 50 g L^{-1}).

monomer conversion of the miniemulsion polymerization initiated by AIBN at 70°C for 4 h was ~ 79%, whereas for the polymerization initiated by KPS was 99%. This may be due to the difference in the initiator nucleation mechanism. Water-soluble initiator, KPS, molecules present in the continuous aqueous phase are capable of not only entering the monomer droplets to form particle nuclei but also promoting homogeneous nucleation, especially for those polymerization systems stabilized by very large amount of surfactant. This is in compliance to Capek's explanation[37]: even with an oil-soluble initiator dissolved in droplets, the nucleation is still dependent on the entry of radicals from the aqueous phase. KPS decomposed and then initiated the polymerization in the aqueous phase. Short chain radicals were first formed in water and then diffused to the monomer droplets or particles to enhance particle size.[38] On the other hand, oil-soluble initiator, AIBN, species experience difficulty in diffusing from the monomer droplets into the aqueous phase; consequently, homogeneous nucleation is greatly retarded. Therefore, to initiate a miniemulsion system containing a high concentration of hydrophobic dye, a water-soluble initiator KPS is most suitable.

Estimation of nanoparticle size by dynamic light scattering

In successful modified miniemulsion polymerization, the droplet size is almost unchanged during and after polymerization because monomer droplets are stabilized by hydrophobe and surfactant. To assess the stability of miniemulsion after polymerization, the particle size measured by TEM and DLS were compared. The number-weighted NICOMP distribution for the prepared nanocolorant, nDR60, under optimum test conditions with highest emulsion stability and smallest particle size was shown in Figure 10. NICOMP particle size distributions for nDR60 consist of a primary peak which in a good agreement with TEM results, and a very small secondary peak which was a result of the bimodal droplet size distribution of starting emulsions. The mean NICOMP diameter for a primary peak of nDR60 particles in the suspension was 13.5 nm.

UV–vis and FTIR spectra of nanocolorant

UV–vis absorption spectra were obtained from the dried nanocolorant dispersed in absolute ethanol and corresponding dyes dissolved in absolute ethanol by using absolute ethanol as a reference solvent. On comparing the maximum absorption wavelength, λ_{max} 588 of nDR60 with λ_{max} 580 nm of DR60, it was found that the λ_{max} of nDR60 showed a hypsochromic shift as in Figure 11. Vis absorption spectra confirmed that, all of the dye is incorporated into the particles.

The absorption energy was shifted to higher frequency with decreasing diameter of the particles.

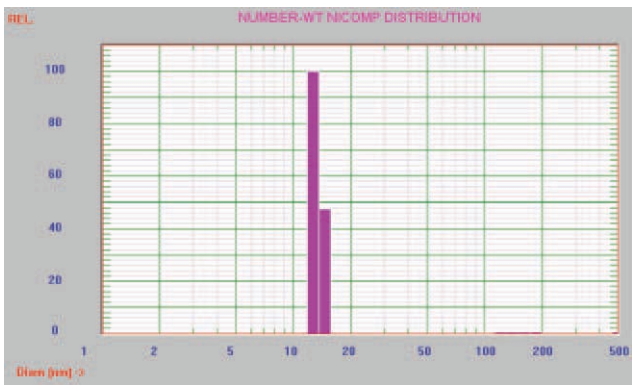

Figure 10 NICOMP particle size distribution of nDR60 suspension (20,000 rpm, 20 min, [nDR60] = 50 g L^{-1}, [SDS] = 80 mmol). [Color figure can be viewed in the online issue, which is available at wileyonlinelibrary.com.]

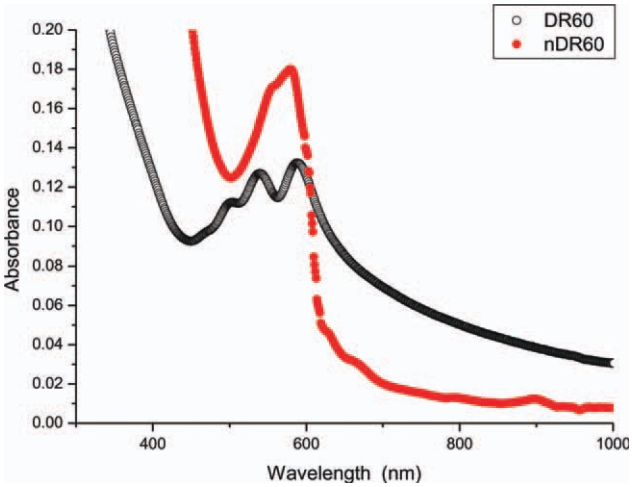

Figure 11 UV–vis absorption spectra of DR60 and nDR60. [Color figure can be viewed in the online issue, which is available at wileyonlinelibrary.com.]

This was readily observed from the reflected color change of particles from blue to red region with increasing the particles size. The red color of DR60 changed from dark red to transparent orange of nDR60 passing through white red and milky pink, where each color correspond to the different particle size of nDR60. Because the anthraquinone-base of dye is a big π conjugated planar structure, it generates intermolecular π–π* interaction and leads to molecular stacking.[39]

The FTIR spectrum of nDR60, Figure 12, showed the same peaks of DR60 together with the specific peaks of PS which are the sp and sp C—H stretching peaks at 3026 and 2924 cm, respectively, as well as the aromatic C=C stretching peak at 1452 cm^{-1}. In addition, the characteristic peaks of PS at 698 and 758 cm^{-1} were observed in the spectrum of nDR60. These peaks indicate the dye was incorporated within the PS particles. Subsequently, these FTIR spectra results proved the chemical composition of nanocolorant particles.

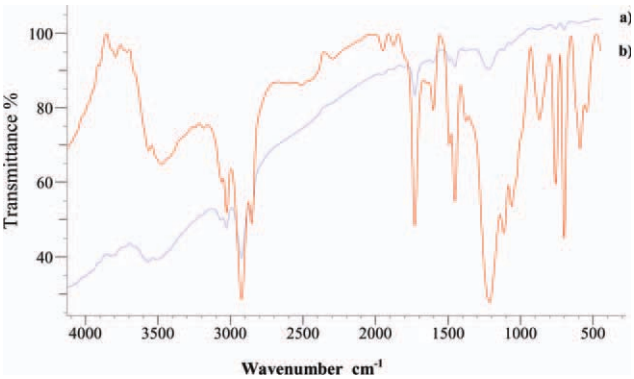

Figure 12 FTIR spectra of (a) DR60 and (b) nDR60. [Color figure can be viewed in the online issue, which is available at wileyonlinelibrary.com.]

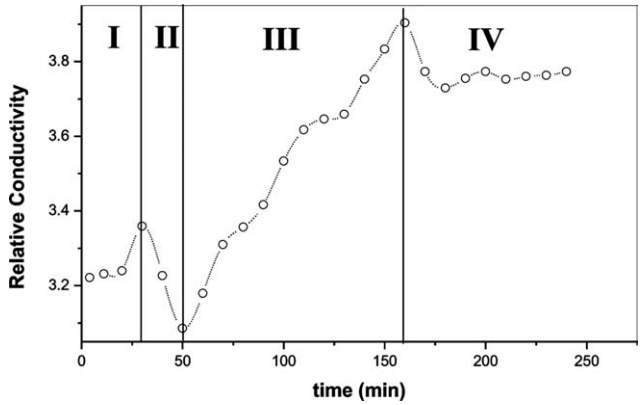

Figure 13 Relative conductivity as a function of time for modified miniemulsion polymerization. I: Radical formation in the aqueous phase by initiator decomposition. II: Polymerization of the radicals in the aqueous phase to give oligomers of increasing hydrophobicity. III: Once the oligoradicals are hydrophobic enough. IV: Monomer droplets may disappear by coalescence with other droplets and polymer particles.

Polymerization kinetic analysis

Mechanism of polymerization

To investigate the particle nucleation mechanism, ascertain the free surfactant concentrations as a function of conductance, indicate the end of the polymerization process. To study the mass transfer of the DR60 from the aqueous phase to the growing latex particles, the polymerization mechanism was further supported by conductivity data shown in Figure 13. It was shown that, particle nucleation occurs during four intervals: the relative conductivity first increased then decreased to minimum and after that increased to maximum as the polymerization proceeds, this was followed by a reduction in the relative conductivity with time. It can be seen that, particle nucleation mechanism involves the following series-parallel processes: the early rise in conductance is corresponding to the addition of an initiator since it is an electrolyte (Interval I).

The decreased conductivity after Interval I is attributed to the formation of primary particles in the aqueous phase. These primary particles require adsorption of sufficient surfactant on the newly created particle surfaces to maintain adequate colloidal stability. This will rapidly deplete the surfactant molecules dissolved in water. In addition, the sodium ions associated with the sulfate ions (derived from the persulfate initiator) may also contribute to the deceased conductivity. The point at which the minimal conductivity occurs marks the end of Interval II.

After the minimal conductivity point was reached, the oligomeric radicals produced in the aqueous phase may either enter the exiting latex particles or penetrate the remaining monomer droplets to convert them into latex particles (Interval III). Furthermore, the growing latex particles may compete with the monomer droplets for monomer and surfactant.

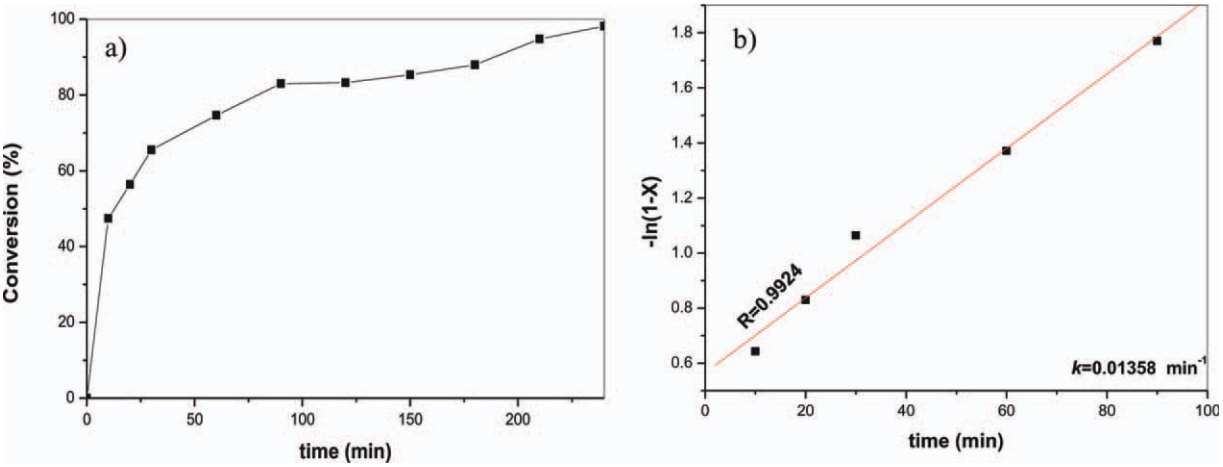

Figure 14 (a) Extent of monomer conversion, (b) pseudo-first order kinetics data for modified miniemulsion polymerization for 4 h. [Color figure can be viewed in the online issue, which is available at wileyonlinelibrary.com.]

Consumption of monomer in the latex particles will cause the monomer molecules to diffuse from the monomer droplets to these reaction loci, even though the hydrophobic dye, DR60, in the monomer droplets offers resistance against such mass transfer process. The adsorbed surfactant may be released from the shrinking monomer droplet surfaces and, thereby increases the conductivity in the aqueous phase. Diffusion degradation of the monomer droplets may also reduce the monomer droplet/water interfacial area and hence contributes to the increased conductivity. The maximum point marks the disappearance of the monomer droplets and the end of Interval III.

Subsequently, the relative conductivity starts to decrease and then level off toward the end of polymerization owing to the depletion of surfactant and perhaps initiator in water (Interval IV).

Rate of polymerization

With sufficiently small particles or a sufficiently large radical flux, the kinetics of miniemulsion polymerization can be described using a pseudofirst-order, where there can be only zero or one radical in a particle at any time and the entry of a radical into the particle will lead to pseudoinstantaneous termination.[40] The monomer conversion percentage versus polymerization time data for the miniemulsion polymerization was shown in Figure 14(a). The maximum conversion percentage for the miniemulsion polymerization was 99%. A first-order kinetic plot of the experimental data was shown in Figure 14(b). The linear region following a short approach to steady-state is indicative of pseudofirst-order kinetics.[41]

Surface tension and surface charge measurements

The chemical and physical behavior of liquids cannot be understood without taking into account surface tension. Surface tension governs the shape that small masses of liquid can assume as well as the degree of contact a liquid can make with another substance. The surface tension of DR60 and nDR60 at 30°C was 59.4 and 39 mN m^{-1}, respectively, and the interfacial tension with benzene was dropped to 42 and 25 mN m^{-1} for DR60 and nDR60, respectively, which indicates the lower surface tension and the rise of surface area for nDR60 than the corresponding DR60.

Zeta potential is the potential difference between the dispersion medium and the stationary layer of fluid attached to the dispersed particle. The significance of zeta potential is that its value can be related to the stability of colloidal dispersions. The zeta potential indicates the degree of repulsion between adjacent, similarly charged particles in dispersion. For molecules and particles that are small enough, a high zeta potential will confer stability, i.e., the solution or dispersion will resist aggregation. When the potential is low, attraction exceeds repulsion and the dispersion will break and flocculate. Therefore, colloids with high zeta potential (negative or positive) are electrically stabilized while colloids with low zeta potentials tend to coagulate or flocculate.

The change in zeta potential of DR60 and nDR60 versus pH range was shown in Figure 15. In the pH range employed, (2–12) the zeta potential of nDR60 was negative, which means the surface is negatively charged. The values of zeta potential were between −40 and −60 mV which ensure that the nDR60 has a good stability at all range of pH. The iso electric point (IEP) was at pH, (1–2) depending on the particle size. This was close to Iler[42] and Wilhelm et al.'s study.[43] While for DR60, it has an excellent stability only in neutral and alkaline media and an incipient instability in acidic medium and the IEP was at pH 3.6.

CONCLUSIONS

A modified miniemulsion polymerization process was successfully used to prepare nDR60 with

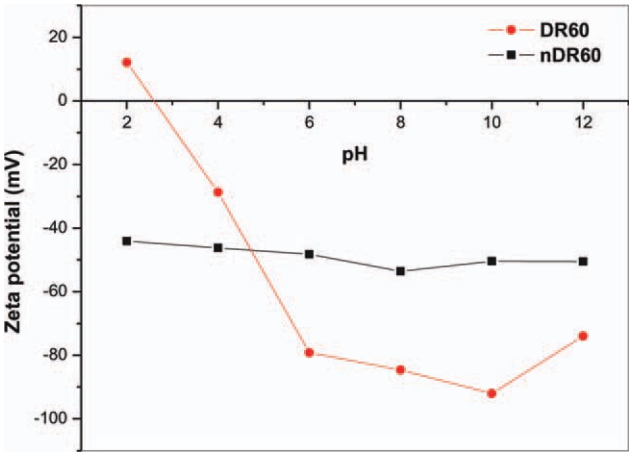

Figure 15 Change in zeta potential of DR60 and nDR60 with pH. [Color figure can be viewed in the online issue, which is available at wileyonlinelibrary.com.]

particle size ~ 8–40 nm. In addition, characterization of nDR60 was investigated by UV–vis spectra which showed a shift to higher frequency with decreasing particles size. FTIR spectra results proved the formation of composite nanoparticles of nDR60. The conductance profiles were found to be a useful tool in describing the various intervals in miniemulsion polymerization. Kinetic analysis of polymerization process was studied by a first-order-kinetic model. The surface tension and surface charge measurements proved that nDR60 has a good stability at all pH range while DR60 has an excellent stability only in neutral and alkaline media and an incipient instability in acidic medium. The work is currently underway to investigate more in depth the application of nanocolorant.

The authors wish to thank Prof. Dr. Azza Hafez for her cooperation to use homogenizer and also they are very grateful to the referees for their useful recommendations and constructive remarks.

References

1. Lanzafame, J. M.; Muenter, A. A.; Brumbaugh, D. V. Chem Phys 1996, 210, 79.
2. Kietzmann, R.; Ehret, A.; Spitler, M.; Willig, F. J Am Chem Soc 1993, 115, 1930.
3. Khazraji, A. C.; Hotchandani, S.; Das, S.; Kamat, P. V. J Phys Chem B 1999, 103, 4693.
4. Ozdemir, O.; Armagan, B.; Turan, M.; Çelik, M. S. Dyes Pigments 2004, 62, 49.
5. Hu, Z. K.; Xue, M. Z.; Zhang, Q.; Sheng, Q. R.; Liu, Y. G. J Appl Polym Sci 2007, 104, 3036.
6. Böhm, A.; Kielhorn-Bayer, S.; Rossmanith, P. Prog Colloid Polym Sci 1999, 113, 121.
7. Widiyandari, H.; Hogan, C. J., Jr.; Yun, K. M.; Iskandar, F.; Biswas, P.; Okuyama, K. Macromol Mater Eng 2007, 292, 495.
8. Ma, Z. Y.; Guan, Y. P.; Liu, X. Q.; Liu, H. Z. Langmuir 2005, 21, 6987.
9. Horak, D.; Benedyk, N. J Polym Sci A Polym Chem 2004, 42, 5827.
10. Yanase, N.; Noguchi, H.; Asakura, H.; Suzuta, T. J Appl Polym Sci 1993, 50, 765.
11. Wang, P. C.; Lee, C. F.; Young, T. H.; Lin, D. T.; Chiu, W. Y. J Polym Sci A Polym Chem 2005, 43, 1342.
12. Liu, X.; Guan, Y.; Liu, H.; Ma, Z.; Yang, Y.; Wu, X. J Magn Magn Mater 2005, 293, 111.
13. Zheng, W.; Gao, F.; Gu, H. J Magn Magn Mater 2005, 293, 199.
14. Liu, Z. L.; Ding, Z. H.; Yao, K. L.; Tao, J.; Du, G. H.; Lu, Q. H.; Wang, X.; Gong, F. L.; Chen, X. J Magn Magn Mater 2003, 265, 98.
15. Schork, F. J.; Luo, Y. W.; Smulders, W.; Russum, J. P.; Butté, A.; Fontenot, K. Adv Polym Sci 2005, 175, 129.
16. Landfester, K. Adv Mater 2001, 13, 765.
17. Landfester, K.; Montenegro, R.; Scherf, U.; Güntner, R.; Asawapirom, U.; Patil, S.; Neher, D.; Kietzke, T. Adv Mater 2002, 14, 651.
18. Asua, J. M. Prog Polym Sci 2002, 27, 1283.
19. Antonietti, M.; Landfester, K. Prog Polym Sci 2002, 27, 689.
20. Huang, C. Y.; Chen, C. M.; Lee, Y. D. Int J Pharm 2007, 338, 267.
21. Samer, C. J.; Schork, F. J Ind Eng Chem Res 1999, 38, 1801.
22. Chern, C. S. A Principles and Applications of Emulsion Polymerization; Wiley: New Jersey, 2008.
23. Faridi-Majidi, R.; Sharifi-Sanjani, N. J Appl Polym Sci 2007, 105, 1244.
24. Xu, Z. Z.; Wang, C. C.; Yang, W. L.; Deng, Y. H.; Fu, S. K. J Magn Magn Mater 2004, 277, 136.
25. Chern, C. S.; Chen, T. J.; Liou, Y. C. Polym 1998, 39, 3767.
26. Haacke, G.; Longordo, E.; Andrawes, F. F.; Campbell, B. H. Prog Org Coat 1998, 34, 75.
27. Liu, X. X.; Yang, J. W.; Chen, Y. L. Polym Adv Technol 2002, 13, 247.
28. Lelu, S.; Novat, C.; Graillat, C.; Guyot, A.; Bourgeat-Lami, E. Polym Int 2003, 52, 542.
29. Takasu, M.; Shiroya, T.; Takeshita, K.; Sakamoto, M.; Kawaguchi, H. Colloid Polym Sci 2004, 282, 740.
30. Takasu, M.; Shiroya, T.; Takeshita, K.; Sakamoto, M.; Kawaguchi, H. Colloid Polym Sci 2003, 282, 119.
31. Landfester, K. Macromol Rapid Commun 2001, 22, 896.
32. Hu, Z.; Xue, M.; Zhang, Q.; Sheng, Q.; Liu, Y. Dyes Pigments 2008, 76, 173.
33. Widiyandari, H.; Iskandar, F.; Hagura, N.; Okuyama, K. J Appl Polym Sci 2008, 108, 1288.
34. Cunningham, M. F. Prog Polym Sci 2002, 27, 1039.
35. Jia, G.; Xu, Y.; Tan, X.; Cai, N. Iran Polym J 2006, 15, 979.
36. Zhang, C.; Wang, Q.; Xia, H.; Qiu, G. Eur Polym Mater 2002, 38, 1769.
37. Capek, I. Adv Colloid Interface Sci 2001, 91, 295.
38. Zhou, X.; Ni, P.; Yu, Z. Polymer 2007, 48, 6262.
39. Kim, J. H.; Matsuoka, M.; Fukunishi, K. Dyes Pigments 1998, 40, 53.
40. Prescott, S. W.; Ballard, M. J.; Gilbert, R. G. J Polym Sci A Polym Chem 2005, 43, 1076.
41. Teo, B. M.; Prescott, S. W.; Ashokkumar, M.; Grieser, F. Ultrasonics Sonochem 2008, 15, 89.
42. Iler, R. K. The Chemistry of Silica; Wiley: New York, 1979.
43. Wilhelm, P.; Zetzsch, C.; Stephan, D. Prog Colloid Polym Sci 2006, 133, 147.